A Multiple-Ring Model for Cognitive Radio Aggregate Interference

Sachitha Kusaladharma and Chintha Tellambura, *Fellow, IEEE*

***Abstract*—This paper proposes a new, flexible, multiple ring model for the aggregate interference analysis of a Poisson field of cognitive radio transmitters distributed over an annular region. For Rayleigh fading or composite Rayleigh fading and Gamma shadowing environments, the moment generating function of the aggregate interference and the exact and asymptotic analysis of the outage are derived for the model. Typically, the model is most accurate for larger guard distances and lower path loss exponents. However, its parameters can be tuned such that a required accuracy is obtained for a trade-off in complexity.**

***Index Terms*—Cognitive radio, aggregate interference, outage probability, shadowing.**

I. Introduction

A POISSON field of cognitive radio (CR) nodes over an annular area with a guard region to reduce interference (Fig. 1.a) has been a popular interference model for underlay CR networks. Several recent works consider this model for their analysis of aggregate interference on the primary system. For example, [1] and [2] propose statistical methods of interference aggregation, while [3] develops a unified framework for deriving interference models, and demonstrates the applicability of predefined distributions for Poisson clustered interferers. A relationship between the outage probability and node density is developed in [4]. Furthermore, aggregate interference modeling has been performed in [5], [6]. References [7], [8] derive the moment generating function (MGF) of the aggregate interference under specific path loss exponents for non-shadowing conditions and Gamma shadowing conditions, respectively. The expressions in [7], [8] are rather complicated because of the need to average over the distributions of node distances, which govern the path loss.

The main objective of this letter is to develop an equivalent ring model that yields simpler analytical results, and which provides flexibility and versatility to handle different parameters. This model is developed to represent the conventional annular system (Fig. 1.a) where the CR nodes are spatially distributed in an annular area. The motivation for this model comes from the mapping theorem [9], where a Poisson process can be mapped to another Poisson process of a lesser number of dimensions. The main benefit of the proposed model is the elimination of averaging over the distance distribution.

This new model consists of M rings of zero width around the primary receiver (PR) (Fig. 1.b). The CR nodes are uniformly distributed on each ring, while their number is a Poisson random variable. The CR node density on the t-th ring is specified by the density β_t ($t = 1, 2 \dots M$). These densities are chosen such that both systems have the same average number of nodes. The MGF of the aggregate interference for this model will be derived under both Rayleigh fading, and composite fading and shadowing. Furthermore, the exact and the asymptotic outage probabilities are derived. The model is shown to be more accurate under certain system conditions, but the approximation error can be kept at user requirements by adjusting model parameters.

Manuscript received November 10, 2013. The associate editor coordinating the review of this letter and approving it for publication was P. Popovski.

The authors are with the Department of Electrical and Computer Engineering, University of Alberta, Edmonton, AB, Canada T6G 2V4 (e-mail: kusaladh@ualberta.ca, chintha@ece.ualberta.ca).

Digital Object Identifier 10.1109/LCOMM.2014.021814.132488

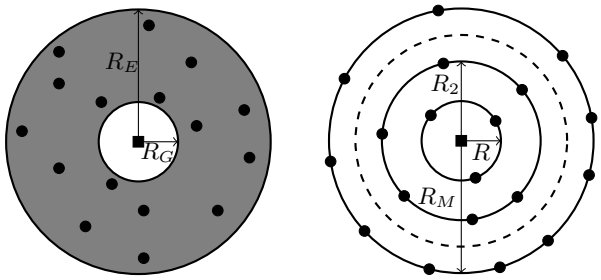

(a) Annular system.

(b) Proposed multiple ring model with the CR nodes on the rings.

Fig. 1: System model. Legend: Black circle = CR nodes, black square = PR, $R_2 = 2R$, and $R_M = MR$.

Notations: $\Gamma(x) = \int_0^\infty t^{x-1}e^{-t}dt$ [10], $f_X(\cdot)$ is the PDF, $F_X(\cdot)$ is the cumulative distribution function (CDF), $M_X(\cdot)$ is the MGF, and $E_X[\cdot]$ denotes expectation with respect to X.

II. Proposed Multiple-Ring Model

The annular system (Fig. 1.a) has a guard region of radius R_G and an outer radius of R_E. The guard region is used to reduce the interference on the PR. Typically, $\frac{R_E}{R_G}$ is taken to be between 3 to 20 [7]. The spatial distribution of interfering nodes is a homogeneous Poisson point process [9], with a node density of β. Furthermore, we consider a time-invariant distribution of CR nodes. For this system, we will develop the new equivalent multiple ring model.

In the proposed model, the CR nodes are distributed in M rings of zero width around the PR (Fig. 1.b). The radius of the t-th ring is tR, where $t = 1 \dots M$. For an annular system, R_E and R_G are given values. Therefore, we must choose R and M accordingly. R is chosen such that it is is a factor of R_G. Therefore, $R_G = \nu R$, where ν is a positive integer less than M. The simplest case arises when $R = R_G$. M is given by $M = \lfloor \frac{R_E}{R} \rfloor$, where $\lfloor \cdot \rfloor$ is the floor function.

The CR nodes in each ring are modeled as a homogeneous Poisson point process. The number of nodes N_t on the t-th ring is independent from the amount of nodes in any other ring, and the probability $P(N_t = n)$ is given by

$$P(N_t = n) = \frac{(\beta_t 2\pi t R)^n}{n!} e^{-\beta_t 2\pi t R}, \quad n = 0, \dots \qquad (1)$$

where t is any integer from 1 to M, and β_t is the CR density of the t-th ring. The density β_t is chosen such that the average

number of CR nodes in the multiple ring model is equal to that of the annular system:

$$\beta(R_E^2 - R_G^2) = \sum_{t=\nu}^{M} \beta_t 2tR. \tag{2}$$

For the homogeneous case, all β_t will be equal ($\beta_t = \beta_l$, $t = \nu \dots M$). For other cases, β_t values will depend on the node intensity profiles and shapes of the interferer distributions.

III. Interference Statistics

We will next derive the MGF of the aggregate interference for the proposed model. This derivation will consider Rayleigh fading or composite Rayleigh fading and Gamma shadowing. These MGF expressions are simple and exact. They can be compared against the exact MGF of the annular system (Fig. 1.a).

The interfering nodes may or may not be transmitting at a given time, and will have an activity factor. This factor can be easily incorporated to our analysis, and thus will not be considered. From the path loss model for large distances, the average interference on the PR from a CR node located a distance r away can be written as $P_{rx} = P_{CR} r^{-\alpha}$, where $P_{CR} = P_0 r_0^{\alpha}$. P_0 is the received power from the CR at a reference distance r_0, and α is the path loss exponent.

Our system model assumes that all the CR nodes are transmitting at the same power level P_{CR}. The total interference power received at the PR may then be written as

$$I = \sum_{t=\nu}^{M} I_t, \tag{3}$$

where I_t is the total interference generated from the CR nodes of the t-th ring. I_t can be expressed as

$$I_t = \sum_{l=1}^{N_t} P_{CR} |h_{t,l}|^2 [tR]^{-\alpha}, \tag{4}$$

where $|h_{t,l}|^2$ is the channel gain corresponding to fading or composite shadowing and fading, for the l-th CR in the t-th ring. The fading and shadowing of CR signals are assumed independent of each other, even for the same ring.

When only Rayleigh fading is considered, $|h_{t,l}|^2$ follows the exponential distribution where $f_{|h_{t,l}|^2}(x) = e^{-x}$. For composite Rayleigh fading and Gamma shadowing, $|h_{t,l}|^2$ has been accurately approximated by a Gamma distribution [11], [12], where the scale and shape parameters θ and k are $\left(\frac{2(\lambda+1)}{\lambda} - 1\right)\Omega_s$ and $\frac{1}{\frac{2(\lambda+1)}{\lambda}-1}$, respectively. It has been shown in [11] that $\Omega_s = \sqrt{\frac{\lambda+1}{\lambda}}$, and $\lambda = \frac{1}{e^{\sigma^2}-1}$, where σ^2 is the variance of corresponding log-normal shadowing. When expressed in the decibel scale, $\sigma_{dB} = 8.686\,\sigma$.

Using eq. (4) in eq. (3), the total interference can be written as

$$I = \sum_{t=\nu}^{M} \sum_{l=1}^{N_t} P_{CR} |h_{t,l}|^2 [tR]^{-\alpha}. \tag{5}$$

A. Rayleigh fading

Under Rayleigh fading, $|h_{t,l}|^2$ values for all t, l are independent and exponential. Therefore, after performing the expectations with respect to $|h_{t,l}|^2$, the MGF $M_I(s) = E[e^{-sI}]$ may be written as

$$M_I(s) = E_{N_t}\left[\prod_{t=\nu}^{M} \frac{1}{\left(1 + sP_{CR}R^{-\alpha}t^{-\alpha}\right)^{N_t}}\right], \tag{6}$$

where the remaining expectation is with respect to $N_1 \dots N_M$. Because the number of CR nodes in the t-th ring is independent of the number of CR nodes in any other ring, we can write eq. (6) as $M_I(s) = \prod_{t=\nu}^{M} E_{N_t}\left[\frac{1}{(1+sP_{CR}R^{-\alpha}t^{-\alpha})^{N_t}}\right]$. After averaging over the distribution (1), the MGF of the aggregate interference can be written as

$$M_I(s) = \prod_{t=\nu}^{M} e^{\beta_l 2\pi tR\left(\frac{1}{1+sP_{CR}R^{-\alpha}t^{-\alpha}}-1\right)}. \tag{7}$$

B. Rayleigh fading and shadowing

When both Gamma shadowing and Rayleigh fading are considered, $|h_{t,l}|^2$ values can be represented by a Gamma PDF. It is assumed that all the $|h_{t,l}|^2$ coefficients are independent. Therefore, after performing the expectations with respect to $|h_{t,l}|^2$ and N_t values, $M_I(s)$ becomes

$$M_I(s) = \prod_{t=\nu}^{M} e^{\beta_l 2\pi tR\left(\frac{1}{(1+\theta sP_{CR}R^{-\alpha}t^{-\alpha})^{k}}-1\right)}. \tag{8}$$

C. Versatility of the model

This subsection will discuss the versatility of the multiple-ring model.

- The incorporation of different transmit powers, path loss exponents, and shadowing variances is complicated with the annular system. Furthermore, non-homogeneous setups and areas with different CR node densities are difficult to analyze. This can be overcome in the multiple-ring model by intelligently substituting β_t instead of β_l, α_t instead of α, and P_t instead of P_{CR} in eqs. (7) and (8). We will not provide further analysis due to space restrictions.
- Moreover, the multiple-ring model may also be used to analyze node distributions of other shapes such as square, hexagon, or linear regions. Again, we will not elaborate further due to space limitations.

IV. Performance analysis

A. CDF of the SINR

Here, we derive the CDF of the signal to interference and noise ratio (SINR). The SINR γ at the PR can be written as $\gamma = \frac{P_p R_{pr}^{-\alpha}|h|^2}{I+\sigma_n^2}$, where P_p is the power level of the primary transmitter (PT), R_{pr} is the distance between the primary transmitter and receiver (the location of the PT does not affect the CR nodes), σ_n^2 is the noise variance, and $|h|^2$ is the channel gain between the primary transmitter and receiver. Due to the mathematical complexity of analyzing for other cases, only the scenario where primary signals undergo path loss and

Rayleigh fading is considered. Then, $|h|^2$ is a unit exponential random variable with $f_{|h|^2}(y) = e^{-y}$ for $y > 0$. Because the variables $|h|^2$ and I are independent, the CDF of γ can be written as

$$F_\gamma(x) = 1 - e^{\left(-\frac{x\sigma_n^2}{P_p R_{pr}^{-\alpha}}\right)} M_I\left(\frac{x}{P_p R_{pr}^{-\alpha}}\right). \quad (9)$$

For Rayleigh fading, substituting (7) for $M_I(s)$ in (9), the CDF of γ becomes eq. (10). Similarly, for Rayleigh fading and Gamma shadowing, substituting (8) for $M_I(s)$ in (9), the CDF of γ becomes eq. (11). Substituting γ_{Th} instead of x yields the outage, where γ_{Th} is the threshold SINR level that the receiver needs.

B. Asymptotic analysis

The asymptotic outage probability under Rayleigh fading, and combined Rayleigh fading and Gamma shadowing is now derived.

First, consider the Rayleigh fading case. For small $\frac{x}{P_p}$, a single product term of (7) can be expanded as $1 - (\beta_l 2\pi t R)\frac{P_{CR}R^{-\alpha}t^{-\alpha}}{P_p R_{pr}^{-\alpha}}x + \mathcal{O}\left(x^2\right)$. By combining this and $e^{-x} = 1 - x$ for small x in (10), we find

$$F_{\gamma_{Asy}}(x) \approx \left(\frac{\sigma_n^2}{P_p R_{pr}^{-\alpha}} + \beta_l 2\pi R \frac{P_{CR}R^{-\alpha}}{P_p R_{pr}^{-\alpha}} \sum_{t=\nu}^{M} t^{1-\alpha}\right) x. \quad (12)$$

Defining $\mathcal{A}_1 = \frac{\sigma_n^2}{P_p R_{pr}^{-\alpha}}$ and $\mathcal{B}_1 = \beta_l 2\pi R \frac{P_{CR}R^{-\alpha}}{P_p R_{pr}^{-\alpha}} \sum_{t=\nu}^{M} t^{1-\alpha}$, we get

$$F_{\gamma_{Asy}}(x) = (\mathcal{A}_1 + \mathcal{B}_1)\, x, \quad (13)$$

which is the asymptotic CDF for the Rayleigh fading scenario.

Similarly, the asymptotic CDF for combined Rayleigh fading and Gamma shadowing can be derived. It can be shown that

$$F_{\gamma_{Asy}}(x) = (\mathcal{A}_2 + \mathcal{B}_2)\, x, \quad (14)$$

where $\mathcal{A}_2 = \frac{\sigma_n^2}{P_p R_{pr}^{-\alpha}}$, and $\mathcal{B}_2 = \beta_l 2\pi R \frac{\theta k P_{CR}R^{-\alpha}}{P_p R_{pr}^{-\alpha}} \sum_{t=\nu}^{M} t^{1-\alpha}$.

V. Numerical Results

This section shows the accuracy and performance of the multiple ring model. The exact and asymptotic variation of the outage probability with respect to the variation of P_p is shown. Simulations are performed for both shadowing and non-shadowing environments to confirm our theoretical results. Moreover, comparisons between the multiple ring model and the annular system are performed. We will use the parameters $\sigma_n^2 = 1$, $P_{CR} = 30$ dB, $\gamma_{Th} = 1$, $R_G = 20$, $R_E = 100$, and $R_{pr} = 30$ for the plots unless stated otherwise. A different R_{pr} would primarily shift the outage probability, and would not affect the overall shape of the curve.

First of all, it is necessary to establish the accuracy of the theoretical results derived for the multiple ring model (eqs. (7), and (8)). In Fig. 2, for varying path loss exponent (α) and shadowing levels (σ), the outage is plotted with respect to the primary power level P_p. The theoretical results match perfectly with the simulations, and as P_p increases, the asymptotic curves coincide with the exact curves. Furthermore, when the path loss exponent increases, Fig. 2 shows that shadowing has little affect on the outage. For the chosen R_{pr}, the outage increases with α, but this may not be the case if R_{pr} had been significantly smaller than R.

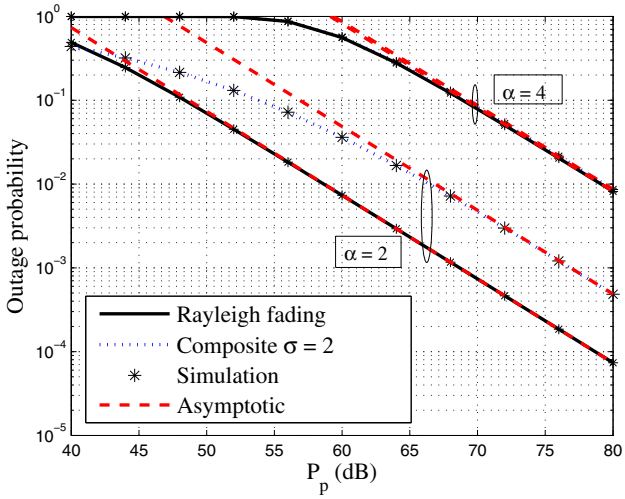

Fig. 2: The exact and asymptotic outage probability vs the normalized transmit power P_p, for different values of σ and α. $\beta_l = 0.01$, $R = 20$, and $M = 5$.

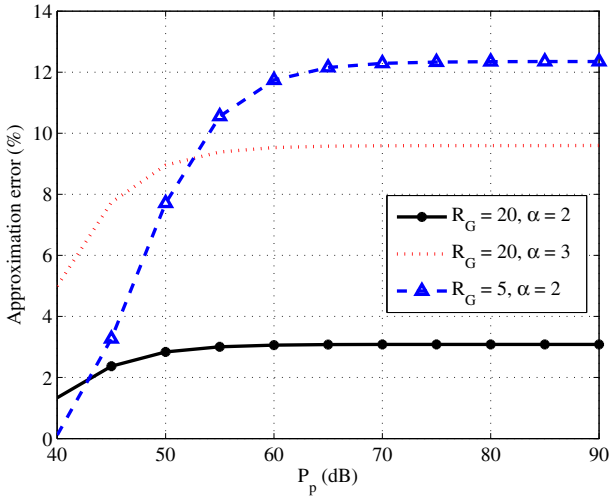

Fig. 3: The percentage error of outage for the multiple ring model vs the normalized transmit power P_p. $\beta = 0.001$, $\sigma = 0$, $\sigma_n^2 = 0$, $R = 5$, and $M = 20$.

The predictive accuracy of the multiple ring model is elaborated in Fig. 3, Fig. 4, and Fig. 5. Fig. 3 investigates the accuracy of the model with regards to the annular system (difference between the prediction's outage (7) and that of the annular system [8]) for different path loss exponent (α) and guard distance (R_G) values. For the node density (β) of 0.001 in the annular system, the corresponding β_l values are obtained from equation (2). The accuracy of the model drops for a given R and M pair with an increase of α or a reduction in R_G. In such a scenario, a larger number of rings should be used in the model (higher M) in order to ensure a required accuracy. The trade-off would be an increase in complexity.

Fig. 4 shows the model's predictive accuracy under different densities. Equation (2) has been used to obtain the corresponding β_l values. The accuracy remains intact for all values of

$$F_{\gamma}^{RF}(x) = 1 - e^{\left(-\frac{x\sigma_n^2}{P_p R_{pr}^{-\alpha}}\right)} \prod_{t=\nu}^{M} e^{\beta_l 2\pi t R \left(\frac{1}{1+\frac{x}{P_p R_{pr}^{-\alpha}} P_{CR} R^{-\alpha} t^{-\alpha}} - 1\right)} \tag{10}$$

$$F_{\gamma}^{Sh}(x) = 1 - e^{\left(-\frac{x\sigma_n^2}{P_p R_{pr}^{-\alpha}}\right)} \prod_{t=\nu}^{M} e^{\beta_l 2\pi t R \left(\frac{1}{\left(1+\theta\frac{x}{P_p R_{pr}^{-\alpha}} P_{CR} R^{-\alpha} t^{-\alpha}\right)^{k}} - 1\right)} \tag{11}$$

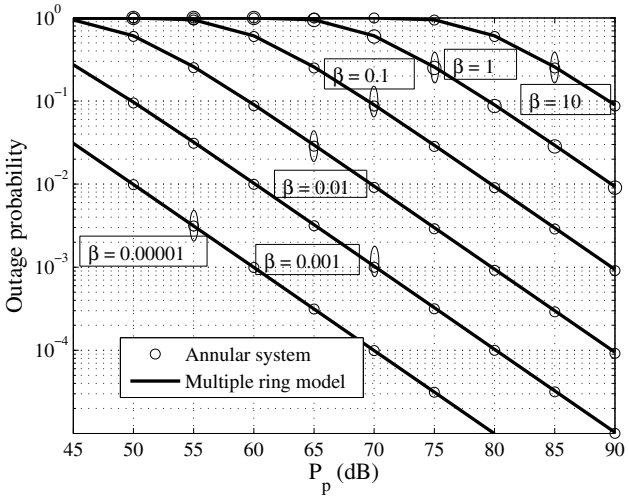

Fig. 4: The outage probability vs the normalized transmit power P_p, under different β, for the annular system and the multiple ring model. $\sigma = 0$, $\alpha = 2$, $R = 5$, and $M = 20$.

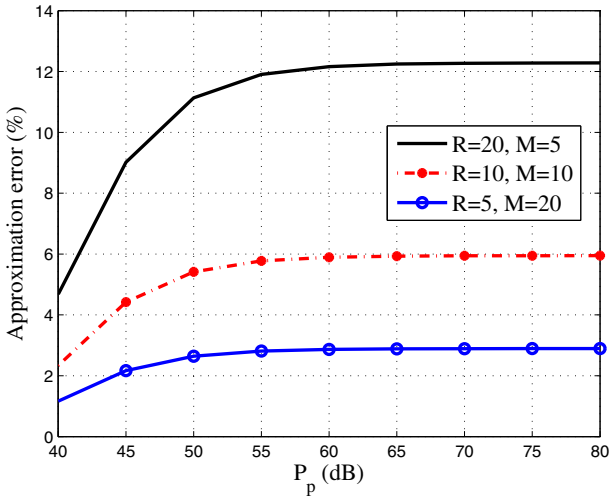

Fig. 5: The percentage error of outage for the multiple ring model vs the normalized transmit power P_p. $\beta = 0.001$, $\alpha = 2$, and $\sigma = 0$.

β considered. A limiting case would be when both the guard distance and node density are small. Nevertheless, changing R and M as necessary will ensure a required error performance.

The predictive accuracy of the multiple ring model for different ring radii is shown in Fig. 5. The error is plotted for different R and M values. The parameters for the annular system are $\beta = 0.001$, a guard distance of 20, and an outer distance of 100. R and M pairs of (20,5), (10,10), and (5,20) are used for comparisons. From (2) the node density β_l for each case will be 0.016, 0.008889, and 0.004706 respectively. For $R = 10$, t is taken from 2 to M, and for $R = 5$, t is taken from 4 to M. The percentage error reduces when the number of rings (M) is increased and vice-versa. With respect to P_p, the percentage errors for all 3 cases rise up to a certain level, and then keeps constant.

VI. Conclusion

To approximate the aggregate interference from a Poisson field of CR nodes over an annular area, a new multiple ring model was proposed. It is parameterized by the distance between the rings, the number of rings, and the node density per ring. The number of interferers per ring is Poisson, and the density parameter is chosen such that the average number of nodes in both the multiple-ring model and the standard annular system match. For Rayleigh and composite fading channels, the exact MGF of the interference, and the exact and asymptotic outage probabilities were derived. The numerical results confirmed the accuracy of the proposed model, which offers enhanced flexibility and mathematically tractability.

References

[1] A. Ghasemi and E. Sousa, "Interference aggregation in spectrum-sensing cognitive wireless networks," *IEEE J. Sel. Areas Commun.*, vol. 2, no. 1, pp. 41–56, Feb. 2008.

[2] A. Rabbachin, T. Q. S. Quek, H. Shin, and M. Z. Win, "Cognitive network interference," *IEEE J. Sel. Areas Commun.*, vol. 29, no. 2, pp. 480–493, Feb. 2011.

[3] K. Gulati, B. Evans, J. Andrews, and K. Tinsley, "Statistics of co-channel interference in a field of Poisson and Poisson-Poisson clustered interferers," *IEEE Trans. Signal Process.*, vol. 58, no. 12, pp. 6207–6222, Dec. 2010.

[4] V. Mordachev and S. Loyka, "On node density–outage probability tradeoff in wireless networks," *IEEE J. Sel. Areas Commun.*, vol. 27, no. 7, pp. 1120–1131, 2009.

[5] Z. Chen, C.-X. Wang, X. Hong, J. Thompson, S. Vorobyov, X. Ge, H. Xiao, and F. Zhao, "Aggregate interference modeling in cognitive radio networks with power and contention control," *IEEE Trans. Commun.*, vol. 60, no. 2, pp. 456–468, Feb. 2012.

[6] X. Hong, C.-X. Wang, and J. Thompson, "Interference modeling of cognitive radio networks," in *Proc. 2008 IEEE VTC – Spring*, pp. 1851–1855.

[7] L. Vijayandran, P. Dharmawansa, T. Ekman, and C. Tellambura, "Analysis of aggregate interference and primary system performance in finite area cognitive radio networks," *IEEE Trans. Commun.*, vol. PP, no. 99, pp. 1–12, 2012.

[8] S. Kusaladharma and C. Tellambura, "Aggregate interference analysis for underlay cognitive radio networks," *IEEE Wireless Commun. Lett.*, vol. 1, no. 6, pp. 641–644, Dec. 2012.

[9] J. F. Kingman, *Poisson Processes*. Oxford University Press, 1993.

[10] I. Gradshteyn and I. Ryzhik, *Table of Integrals, Series, and Products*, 7th ed. Academic Press, 2007.

[11] I. Kostic, "Analytical approach to performance analysis for channel subject to shadowing and fading," *IEEE Proc. Commun.*, vol. 152, no. 6, pp. 821–827, Dec. 2005.

[12] S. Al-Ahmadi and H. Yanikomeroglu, "On the approximation of the generalized-K distribution by a gamma distribution for modeling composite fading channels," *IEEE Trans. Wireless Commun.*, vol. 9, no. 2, pp. 706–713, Feb. 2010.